Journal of Electromagnetic Waves and Applications

ISSN: 0920-5071 (Print) 1569-3937 (Online) Journal homepage: http://www.tandfonline.com/loi/tewa20

Hemisphere lens-loaded Vivaldi antenna for time domain microwave imaging of concealed objects

Zubair Akhter, Abhijith B. N. & M. J. Akhtar

To cite this article: Zubair Akhter, Abhijith B. N. & M. J. Akhtar (2016) Hemisphere lens-loaded Vivaldi antenna for time domain microwave imaging of concealed objects, Journal of Electromagnetic Waves and Applications, 30:9, 1183-1197, DOI: 10.1080/09205071.2016.1186574

To link to this article: http://dx.doi.org/10.1080/09205071.2016.1186574

JOURNAL OF ELECTROMAGNETIC WAVES AND APPLICATIONS, 2016
VOL. 30, NO. 9, 1183–1197
http://dx.doi.org/10.1080/09205071.2016.1186574

Taylor & Francis
Taylor & Francis Group

Hemisphere lens-loaded Vivaldi antenna for time domain microwave imaging of concealed objects

Zubair Akhter[a], Abhijith B. N.[b] and M. J. Akhtar[a]

[a]Department of Electrical Engineering, Indian Institute of Technology, Kanpur, India; [b]Department of Electronics Engineering, Rajiv Gandhi University of Knowledge Technologies, Kadapa, India

ABSTRACT

The hemisphere lens-loaded Vivaldi antenna for the microwave imaging applications is designed and tested in this paper. The proposed antenna is designed to work in the wide frequency band of 1–14 GHz, and is fabricated on the FR-4 substrate. The directivity of the proposed Vivaldi antenna is enhanced using a hemispherical shape dielectric lens, which is fixed on the end-fire direction of the antenna. The proposed antenna is well suited for the microwave imaging applications because of the wide frequency range and high directivity. The design of the antenna is carried out using the CST microwave studio, and various parameters such as the return loss, the radiation pattern, the directivity, and input impedance are optimized. The maximum improvement of 4.19 dB in the directivity is observed with the designed hemisphere lens. The antenna design is validated by fabricating and testing it in an anechoic environment. Finally, the designed antenna is utilized to establish a setup for measuring the scattering coefficients of various objects and structures in the frequency band of 1–14 GHz. The two-dimensional (2D) microwave images of these objects are successfully obtained in terms of the measured wide band scattering data using a novel time domain inverse scattering approach, which shows the applicability of the proposed antenna.

ARTICLE HISTORY
Received 24 April 2015
Accepted 29 April 2016

KEYWORDS
Active microwave imaging; free space imaging method; inhomogeneous media; non-destructive testing; remote sensing; time domain reconstruction; through wall imaging; Vivaldi antenna

1. Introduction

Presently, there is a lot of interest to use the microwave imaging technology as an alternative to the standard X-ray scanners to secure public places. There a number of reasons to use the microwave technology in lieu of the conventional X-ray technology in recent years. The first and foremost reason is the advent of plastic and non-metallic hazardous explosives, which cannot be quite efficiently detected using the X-ray scanners as they were primarily designed for the detection of metals. The microwaves, on the other hand, have the capability to detect various plastic and non-metallic explosives as each of these objects would usually show distinct permittivity values. The second reason for the microwave technology receiving much attention in recent years is due to the safety issues as the microwaves are non-ionizing

CONTACT Zubair Akhter zuakhter@iitk.ac.in

radiations thus posing no serious health hazard to persons. The above-mentioned factors leads researchers to explore the possibilities of microwave imaging in number of industrial applications such as imaging of concealed objects, detection of anti-personnel mines, through wall imaging, and biomedical applications.[1–3] For detection of contraband and imposter objects, various imaging systems are installed at security locations which ultimately produce two-dimensional (2-D) image of a scene, person, or object. The radio frequency (RF)/microwave imaging systems usually require the wide-band highly directional antennas along with other associated RF components to measure the scattering (*S*-parameters) data of the test media. The measured *S*-parameters are then utilized in association with some appropriate reconstruction algorithm to obtain a stable microwave image of the test medium.[4] The ultra-wide band (UWB) antennas having high directivity are desirable to obtain a good spatial and axial resolution image of the test media.[5] The Vivaldi antenna is an excellent choice for various microwave imaging applications such as the breast tumor detection, the through wall imaging, etc. because of its UWB characteristic.[6–8] The Vivaldi antenna is basically a tapered slot traveling wave antenna having wide operating frequency band due to its frequency-independent radiating characteristic.[9,10] Conventionally, the Vivaldi antennas are slot-line type, either employing a microstrip line to slot-line transition or a balun using $\lambda/4$ transmission line sections, which limits its operating bandwidth. The development of antipodal Vivaldi antenna, which can be directly fed from a coaxial connector, reduces the complexities in the transition design, and overcomes the high frequency limitation.[10] The depth dependence microwave imaging of the dielectric media usually requires the wide-band reflection coefficient data starting from a very low frequency.[11] Hence, an UWB antenna with lower frequency limit well below the standard Vivaldi antennas [12] is required for such applications. The lower frequency operation of the Vivaldi antenna is primarily limited by its width which should be greater than $\lambda_{max}/2$, with λ_{max} being the free space wavelength corresponding to the lowest frequency of operation. For microwave imaging applications, the directivity of the antenna should be quite high (typically of the order of 10 dB in the higher frequency range). The higher directivity results into narrow beamwidth of the antenna which provides a better resolution in the lateral direction of the obtained microwave image of the test media. On the contrary, the axial resolution of the obtained microwave image can be improved by increasing the scanning bandwidth. From the practical point of view, the scanning bandwidth would always be limited due to the fact that the antenna and other RF components would be working only over a limited frequency range. Now, in order to improve the directivity of Vivaldi antennas, various techniques have been proposed in literature, which include circular shape-load and slot-load,[13] Zero Index Metamaterials,[14] and a director at the aperture of the antenna.[15] To the best of author's knowledge, the use of hemisphere dielectric lens to increase the directivity of Vivaldi antenna has not been presented earlier in the literature. The preliminary design of a simple wide band antipodal Vivaldi antenna with the lower frequency range starting from 1 GHz has earlier been proposed.[16] The directivity of the earlier proposed antenna is, however, not adequate for the microwave imaging applications.

The aim of this paper is twofold. In the first step, the design of a simple Vivaldi antenna is refined, and various design parameters are optimized. Afterwards, a hemisphere dielectric lens is proposed to improve the directivity and beamwidth of the Vivaldi antenna in the designated frequency band. The designed antipodal Vivaldi antenna loaded with the hemisphere dielectric lens is then fabricated and tested in the frequency range of 1–14 GHz. The

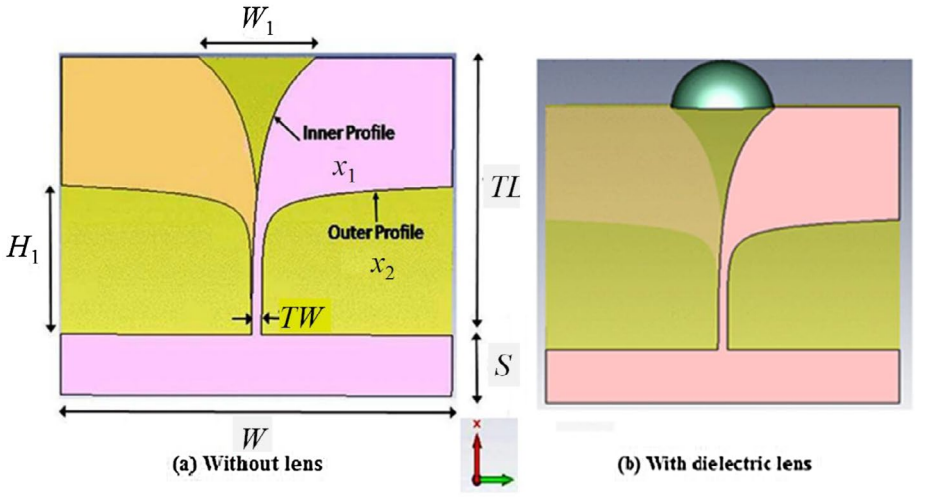

Figure 1. Geometry of the designed Vivaldi antenna.

performance of the designed antenna is found to be substantially improved for the microwave imaging applications after optimizing various parameters. The second step here involves utilizing the designed antenna in the microwave imaging setup to investigate various real-life contraband detection problems. In this framework, the 2D microwave images of various objects are obtained in terms of the measured scattering data by making use of the proposed novel time domain inverse scattering approach. It is to be noted that the time domain inverse scattering approach has usually been applied till now to obtain the one-dimensional (1-D) permittivity profile of simple stratified media.[17,18] However, in this paper, the time domain approach has been applied for the first time to obtain 2-D microwave images of the test media using the proposed lens-loaded Vivaldi antenna. It is also observed that the proposed technique is able to image the objects using electromagnetic waves of even larger wavelengths (i.e. 1–14 GHz) as compared to conventional mm/THz imaging systems due to the improved focusing capability of the hemisphere lens.

2. Design of the hemisphere-loaded Vivaldi antenna

The proposed antenna consists of two copper layers etched on the FR-4 substrate as shown in Figure 1, where both ground and conductor planes are flared exponentially. The feeding part is similar to a microstrip line whose width is adjusted to obtain input impedance close to 50 Ω. The antenna is fed through a SMA connector to the micro-strip line which then continues as a twin-line. The flares can be considered as tapered slot line except for the fact that the two metallization layers are on different plane.

The final design of the antenna is achieved by a detailed parametric analysis of various parameters such as, the width of the antenna (W), the exponential taper profile amplitudes A_1 and A_2 the opening of the flares (W_1), the taper length (TL), the inner profile height (H_1), and the feed line length (S). A flexible design equation is proposed here, which is used to obtain the initial design parameters of the proposed antenna. The taper profiles (x_1, x_2) and taper rates (r_1, r_2) of the proposed Vivaldi antenna can be given as

$$x_1 = A_1\left(e^{yr_1^{n_1}} - 1\right) - \frac{TW}{2} \tag{1}$$

$$x_2 = A_2\left(e^{yr_2^{n_2}} - 1\right) - \frac{TW}{2} \tag{2}$$

$$r_1 = \frac{\log\left(\frac{W_1 + A_1 + \frac{TW}{2}}{A_1}\right)}{H^{n_1}} \tag{3}$$

$$r_2 = \frac{\log\left(\frac{W + A_2 + \frac{TW}{2}}{A_2}\right)}{H_1^{n_2}} \tag{4}$$

where, the exponent terms n_1 and n_2 are taken as 2 and 5, respectively.

It can be seen from above equations that the taper rates are depending on the dimensions of the antenna as well as on the taper flare amplitudes (A_1, A_2). The line width (TW) is chosen such that the input impedance of the antenna is approximately equal to 50 Ω. The shape of the designed antenna is considered to be consistent as long as $H > H_1 = TL$ and $W > W_1$. After obtaining the initial sets of parameters using the above sets of analytical equations, the numerical simulation of the antenna geometry is carried out using the CST microwave studio. A detailed parametric analysis is carried out for various antenna parameters, which are optimized for the desired performance. The fabrication of the designed antenna is carried out on the FR-4 substrate with relative permittivity of 4.3 having thickness of 1.6 mm. The optimization goals have been set to obtain the lower cut-off frequency close to 1 GHz, and the upper cut-off frequency above 14 GHz.

2.1. Parametric analysis

The lower frequency of operation of the Vivaldi antenna is mainly decided by its width (W). Therefore, this parameter should be at least half the highest wavelength in the operating frequency band. However, the width of antenna can't be increased beyond a limit as increasing the width reduces the directivity of the designed antenna even in the higher frequency range. The reduction of directivity in turn decreases the lateral resolution of the obtain microwave image which adversely affects the overall imaging scheme. Moreover, increasing the width of the antenna increases its overall size. Hence, the selection of width (W) is a compromise between the lowest frequency of operation and the directivity. The change in the antenna reflection characteristic in the designed frequency band as a function of width (W) of the antenna is shown in Figure 2.

It can be observed from this figure that the lower cut-off frequency satisfying the 10 dB return loss criterion can be taken as around 1 GHz only under those situations where the width W of the antenna is taken as 112 mm or more.

Meanwhile, it can be seen from Figure 3 that the high frequency response does not change much due to variation in the flare opening width (W_1), but the lower frequency return loss is increased for lower values of W_1. However, the flare opening mainly decides the matching of the antenna to the free space, and hence this parameter cannot be increased much to improve the low frequency response. Thus, a trade-off is to be obtained for the parameter

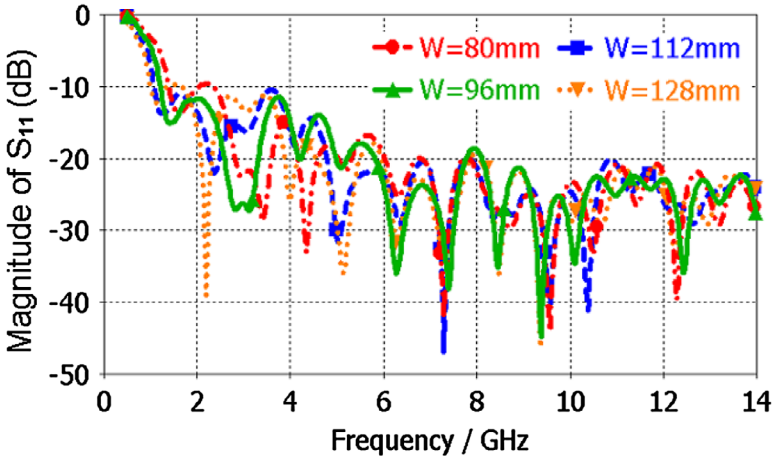

Figure 2. Variation of S_{11} with the total antenna width W with $TL = 80$ mm, $W_1 = 36$ mm, $H_1 = 42$ and $S = 18$ mm.

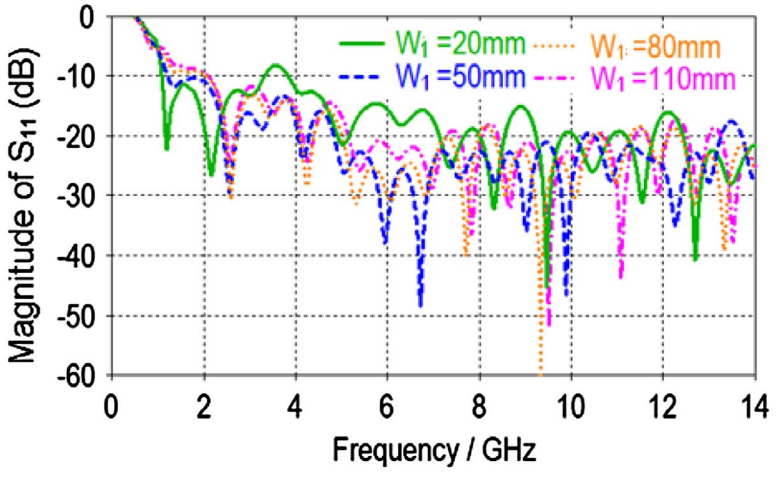

Figure 3. Variation of S_{11} with flare opening width W_1 with $W = 110$ mm, $TL = 80$ mm, $H_1 = 42$ mm and $S = 18$ mm.

W_1 in order to improve the lower frequency return loss without affecting the matching significantly in the higher frequency range.

The taper length of the antenna should be half a wavelength at the lowest operating frequency to radiate effectively in the designated frequency band. It basically means that at this frequency, the designed antenna should satisfy the 10 dB criterion. Now, it can be observed from Figure 4 that for antennas having TL of 80 mm or less, the return loss is less than 10 dB in the lower frequency range around 1 GHz. However, increasing this parameter beyond a certain value would increase the antenna dimensions. Hence, again a trade-off is to be obtained.

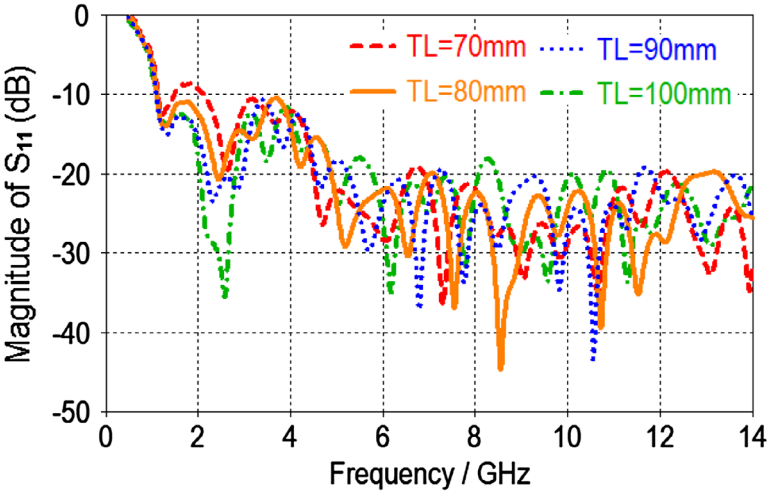

Figure 4. Variation of S_{11} with taper length *TL* with $W = 110$ mm, $W_1 = 36$ mm, $H_1 = 42$ mm and $S = 18$ mm.

2.2. Directivity improvement

The microwave imaging usually requires the focused beam to profile the media under test in order to improve the resolution. To accommodate lower frequencies, the antenna dimensions should be increased which causes a wider beam. Thus, it is important to have a directing structure to improve the beam forming of the antenna. A dielectric lens is found to be focusing the beam well, which actually improves at higher frequencies.

A Teflon hemisphere has been used here for creating a dielectric lens. A groove is cut on the upper flat surface of the hemisphere to attach it to the antenna. Figure 5 shows the structure and dimensions of the proposed dielectric lens. In the simulation result, the directivity is found to be increased by 1–4 dBi at higher frequencies.

The simulation studies are done with the hemispheres of various sizes. The directivity enhancement is better when the diameter of the lens is higher. However, the higher size would also increase the weight of the structure. The parametric analysis is done here by comparing the input reflection coefficient of the antenna at different diameters of the hemisphere since it affects the reflection coefficient at lower frequencies.

A plot of directivity vs. frequency for various radius of the hemisphere dielectric lens is shown in Figure 6. It is obvious from this plot that the directivity enhancement is better at higher frequencies and at higher diameter of the hemisphere. It should also be noted from this figure that the directivity of the antenna with lens for all radii values is much higher than the no lens case. However, the reflection coefficient of the antenna and the feasibility of design are to be considered here for selecting the lens. The best value of radius for the lens made of Teflon is found to be 24 mm after parametric analysis which makes the return loss in the entire frequency band (i.e. 1–14 GHz) less than 10 dB. There is a considerable improvement in the beam width of the antenna, and the beam gets more focused if the proposed lens is used in combination with the designed Vivaldi antenna.

Based on the outcome of the detailed parametric analysis, the final dimensions of the antenna are selected for the desired frequency range, i.e. 1–14 GHz as given in Table 1. The antenna with this selected set of parameters provides good results for microwave imaging application.

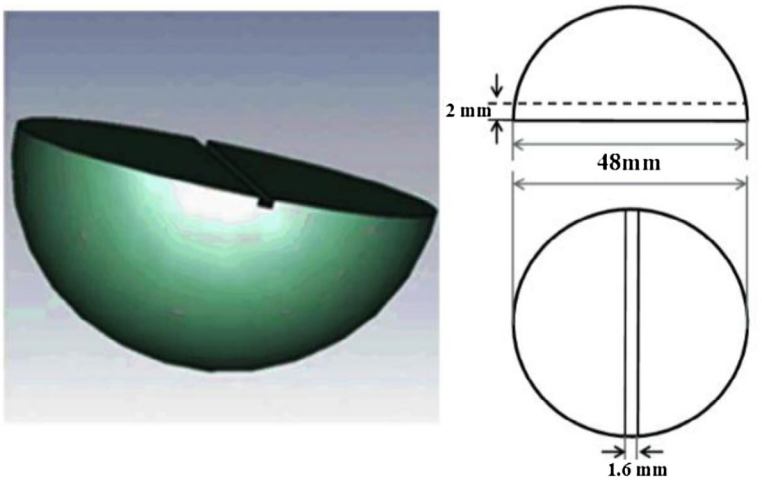

Figure 5. Hemisphere dielctric lens.

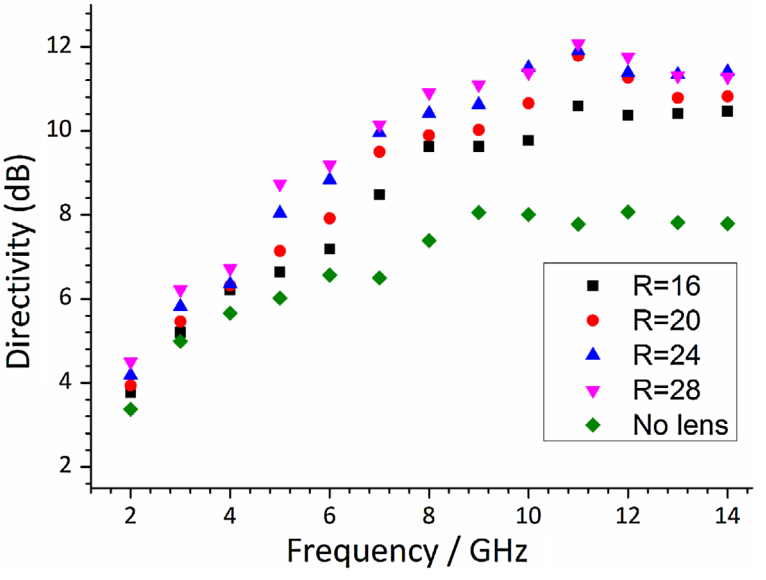

Figure 6. Comparison of directivity in case of no lens to various lens radius.

2.3. Measured performance of antenna

The designed antenna is fabricated on the FR-4 substrate for testing and validation. The SMA connector is soldered with the support of a ground base, and the measurements are taken using the Agilent (N5230C) Vector Network Analyzer (VNA).

Figure 7 shows the comparison between the simulated and the measured input reflection coefficient of the designed antenna loaded with hemisphere lens. It can be observed from this figure that the measured bandwidth is greater than 13 GHz, which matches with the simulation result.

Table 1. Final dimensions of the designed antenna (mm).

W	TL	W_1	H_1	TW	n_1	n_2	A_1	A_2	R
110.3	82.2	36.4	42.9	2.9	2	5	1.6	1.2	24

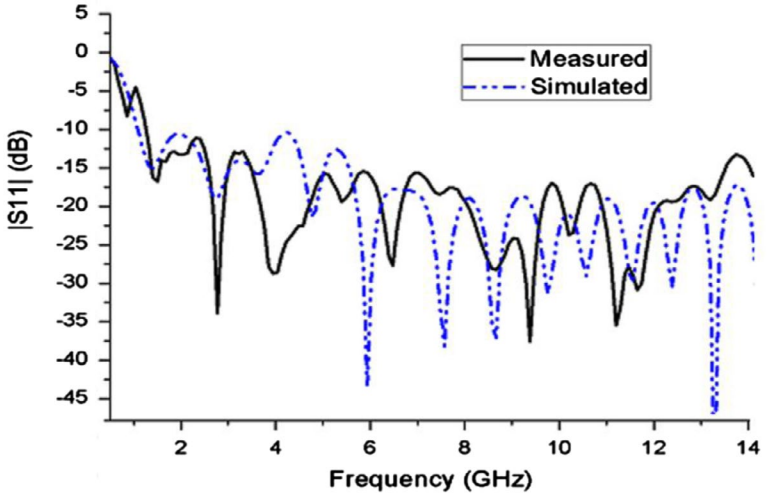

Figure 7. Comparison of simulated and measured S_{11} of the designed Vivaldi antenna.

The comparison of directivity and peak realized gain of the designed antenna with and without hemisphere lens structure is given in Figures 8 and 9, respectively. From Figure 8, it is evident that the directivity of the designed antenna loaded with hemisphere dielectric lens as compared to reference antenna (without lens) is improved significantly. It is also observed that the improvement in directivity is quite substantial in the higher frequency range viz. 6–12 GHz. The above results also indicate that the utilization of hemisphere lens along the aperture of the antenna will lead to higher directivity, and around 4.19 dB improvement in directivity is observed as compared to the reference antenna.

The effect of dielectric lens is also studied by measuring the peak realized gain at different frequencies. Two identical standard wide band horn antennas (Q-par Angus Ltd.) are used as reference antennas during gain measurement in an anechoic chamber. It is evident from Figure 9 that the use of the dielectric lens increases the gain of the designed Vivaldi antenna by around 3 dB. The use of the dielectric lens shows similar behavior in the electric field pattern as shown in Figure 10. It is evident from these figures that the directivity of the antenna is significantly improved using the dielectric lens. The radiation patterns of the fabricated antenna have been measured in the anechoic chamber as shown in Figure 11. The improvement of the directivity with dielectric lens is observed more at higher frequencies as compared to the lower frequency range.

3. Proposed time domain microwave imaging scheme

In past, various approaches has been proposed for contraband detection mainly targeted for homeland security and biomedical applications.[19–23] In most of the situations, the overall microwave imaging scheme is compromise between the complexity involved and

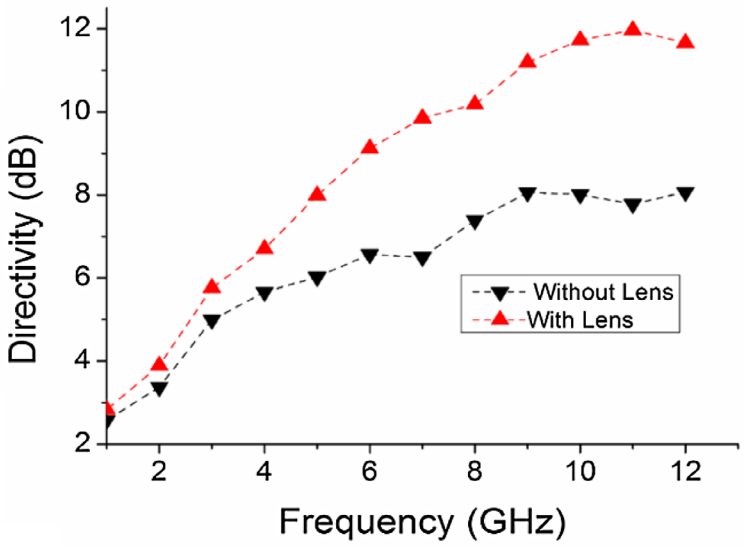

Figure 8. Comparison of directivity with and without dielectric lens.

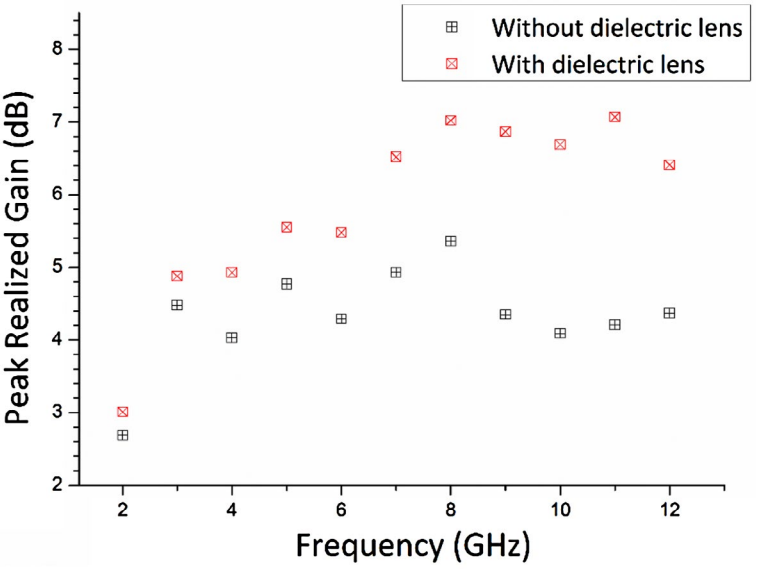

Figure 9. Comparison of measured peak realized gain with and without dielectric lens.

the quality of image obtained using the particular procedure. In this paper, our main focus is to reduce the complexity and cost of the overall microwave imaging scheme without compromising much on the image quality. This is facilitated by proposing noniterative time domain-based reconstruction algorithm, and making use of the designed wide band Vivaldi antenna with improved directional properties. In this section, the designed antenna is actually employed to scan the test object in order to measure the scattering data at various positions. The 2-D microwave image of these objects are then obtained in terms of the

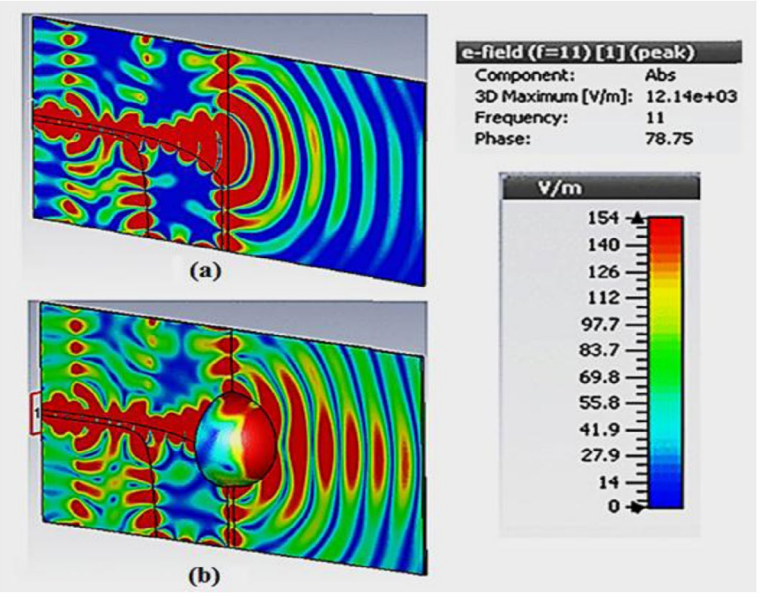

Figure 10. (a) Electric field distribution without hemisphere dielectric lens at 11 GHz. (b) Electric field distribution with hemisphere dielectric lens at 11 GHz.

measured scattering data using a novel time domain inverse scattering approach, which can be considered to be modified version of the recently proposed 1-D imaging scheme. [17] The background medium is assumed to be air, which means that the system experiences a step change in permittivity at the position of the medium under test (MUT) as shown in Figure 12. In this figure, the center of each grid represents the sensor location. It is to be noted that under practical situation, each sensor location would be replaced by a narrow beam antenna, which would be connected to VNA. The plane wave approximation is assumed to be valid at the scanned location. For satisfying these condition, a focusing lens antenna is employed so that the separation between the points $z = 0$ and $z = l$ can be kept low.

The scattering data are collected at each antenna/sensor location. The amount of reflectivity over *xy* plane at each sampling point is determined using an equivalent time domain technique described in later part of this article. The 2-D qualitative dielectric image of the test media at the interface is generated by plotting the spatial permittivity values obtained at each sampling location using the proposed approach. The *imresize* function of MATLAB is used to refine the obtained dielectric image,[24] where one can differentiate various regions based on their permittivity values. The obtained dielectric image of the test media can ultimately be used to locate/identify the concealed objects by distinguishing them from the background medium.

3.1. Image reconstruction algorithm

It has been assumed here that media is flat and EM wave is incident normally on the media under investigation. The steps involving for generating the dielectric image are outlined in following steps.

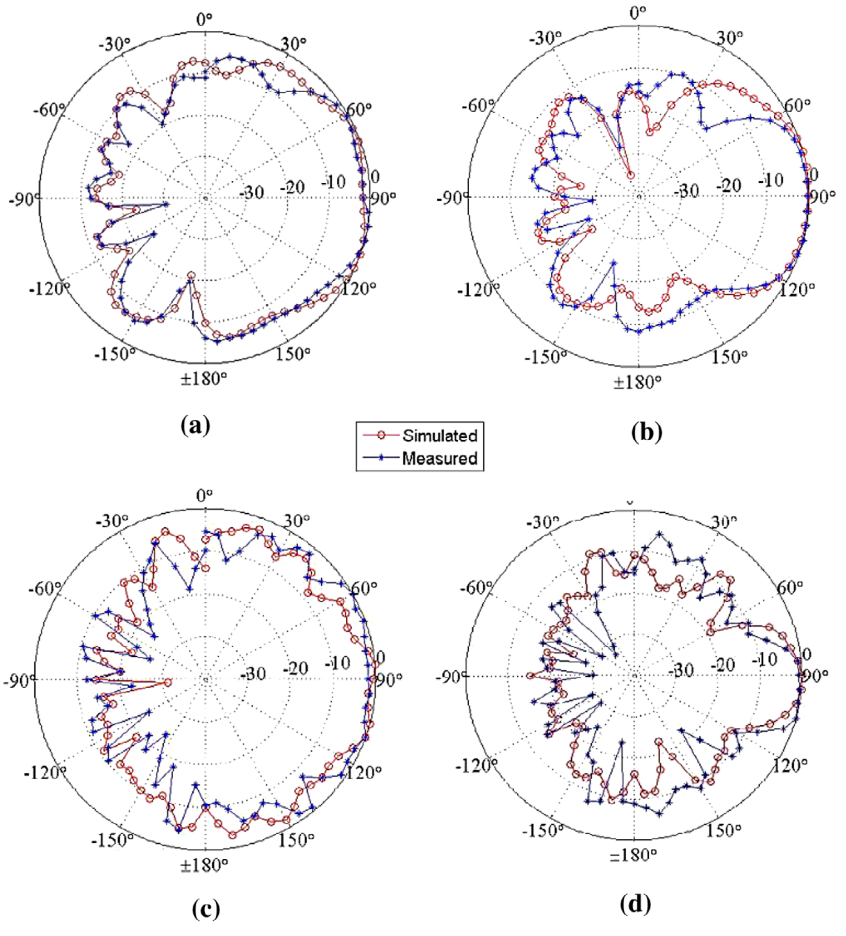

Figure 11. Measured and simulated E-field radiation pattern of designed antenna (a) without lens at 6 GHz, (b) With lens at 6 GHz, (c) Without lens at 12 GHz, and (d) With lens at 12 GHz.

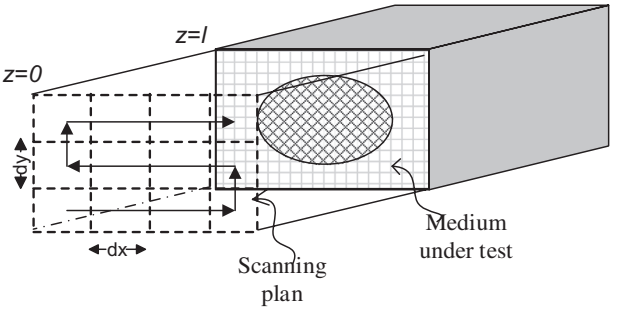

Figure 12. Imaging system configuration and scanning mechanism.

Step1: The metal plate is placed over the surface of MUT, and the *S*-parameters in the specified frequency band are measured. The band limited inverse fast Fourier transform is applied on the measured S_{11} data, and the resultant reflected signal in equivalent time

domain is recorded for reference. The metal plate of larger cross-sectional dimension is taken here so that it fully covers the MUT thereby eliminating the need of placing a small metal plate at every measurement/pixel location.

Step 2: After removing the metal plate, the scanning of test media over *xy*-plane is carried out using the proposed antenna and the associated RF components. The scanning provides the measured scattering data at each grid point as shown in Figure 12.

Step 3: The qualitative normalized permittivity/reflectivity image with improved contrast variation is generated on the basis of reference reflectivity (when MUT is completely covered by the metal plate) and the inherent reflectivity ($\mathfrak{R}$) from the surface of MUT.

$$\mathfrak{R} = \left|\Gamma_{(n,m)}\right|^2 = \frac{P_{r(n,m)}}{P_{i(n,m)}} \tag{5}$$

$$\varepsilon_{r(n,m)} = \varepsilon_{r0}\left(\frac{1+\left|\Gamma_{(n,m)}\right|}{1-\left|\Gamma_{(n,m)}\right|}\right)^2 \tag{6}$$

where $P_{i\,(n,m)}$ and $P_{r\,(n,m)}$ are the local incident and the reflected normalized powers at each pixel represented by the *n*th row and *m*th column in the overall measurement matrix. From the above-mentioned technique, the reflectivity variation which is related to permittivity variation of the MUT at the interface plane, is measured and presented in the form of 2D images.

3.2. 2-D imaging results

First of all, the 2-D microwave image of a typical laboratory made standard as shown in Figure 13 is obtained to validate the performance of the designed antenna for practical imaging applications. The laboratory standard consists of two metal patches of triangular and rectangular shapes being etched over the FR-4 substrate of known dimensions as shown in Figure 14(a). The actual measurement includes the proposed antenna along with the VNA, and the measurements of scattering parameters are carried out at each sampling location in the frequency range of 1–14 GHz. The. In this case, the measurement of reflection coefficient S_{11} is done at 17 (row) × 28(columns) sampling locations having the separation of 200 mm between antenna and MUT. After applying the proposed imaging algorithm, a corresponding reflectivity images are generated, which are further refined with the help of MATLAB-based algorithm as shown in Figure 14(b) and (c).

Figure 14(b) represents the microwave image of the object shown in Figure 14(a) obtained with the help of deigned antenna without lens being present. It can be clearly observed that both the structures are not clearly distinguishable in Figure 14(b) because of relatively low directivity of the Vivaldi antenna in this case. It is mainly due to this reason that the standard Vivaldi antenna is loaded with the designed hemisphere lens, and Figure 14(c) shows the microwave image of the same object obtained with the help of lens-loaded Vivaldi antenna. From Figure 14(c), it is obvious that the two structures can now be clearly distinguished in comparison to the background medium. After comparing Figure 14(c) with that of 14(a), it can be concluded that the two structures of different shapes can be identified, and their relative positions can also be approximately determined with the help of the designed Vivaldi antenna loaded with the hemisphere lens.

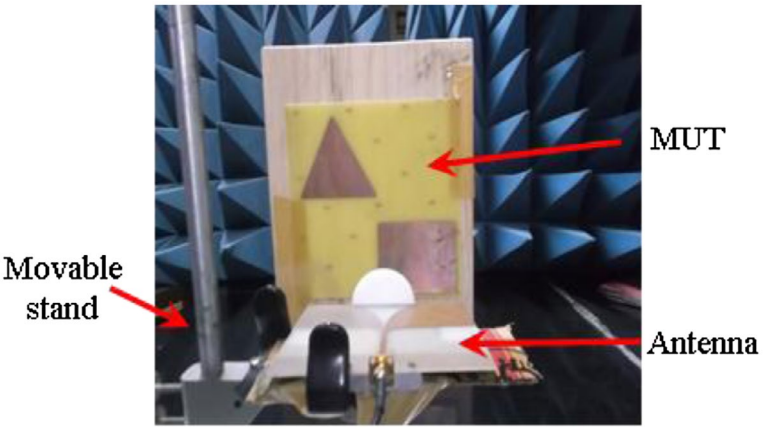

Figure 13. Practical imaging system setup configuration.

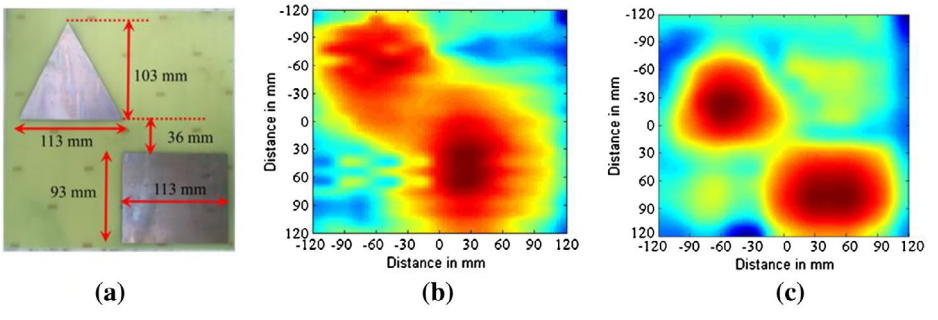

Figure 14. (a) FR-4 sheet etched with triangle and rectangle. (b) Corresponding reflectivity image obtained using the proposed scheme without lens. (c) Corresponding reflectivity image obtained using the proposed scheme with lens.

In the second case, a mannequin with a gun shaped metallic concealed object is considered as shown in Figure 15. The measurement of reflection coefficient is done using the lens antenna in a similar fashion as described earlier at 14 (rows) × 14(columns) sampling locations having the separation of 200 mm between antenna and MUT in the region specified by rectangle shown in Figure 16(a).

Figure 16(b) shows the presence of a concealed structure which can be clearly distinguished from the background medium. In this case because of the limited resolution, the shape information cannot be very accurately obtained. However, the presence of an object concealed behind the cloth having different dielectric signature as compared to the background medium has been identified successfully.

Conclusion

In this work, a novel antipodal Vivaldi antenna has been designed, fabricated and tested. The directivity of the antenna ranges from 2.4 to 11.46 dBi in the wide-band frequency range starting from 1.05 to 14 GHz. The return loss of the antenna is well above 10 dB in the entire

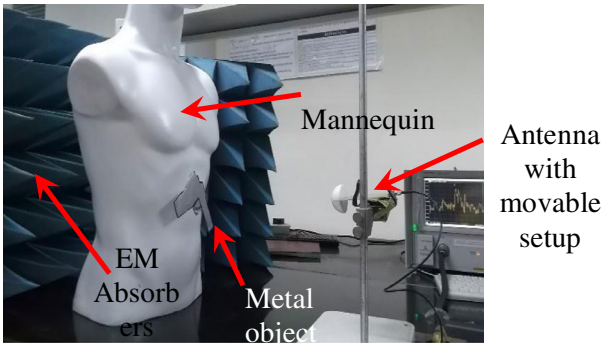

Figure 15. Imaging system configuration and scanning mechanism.

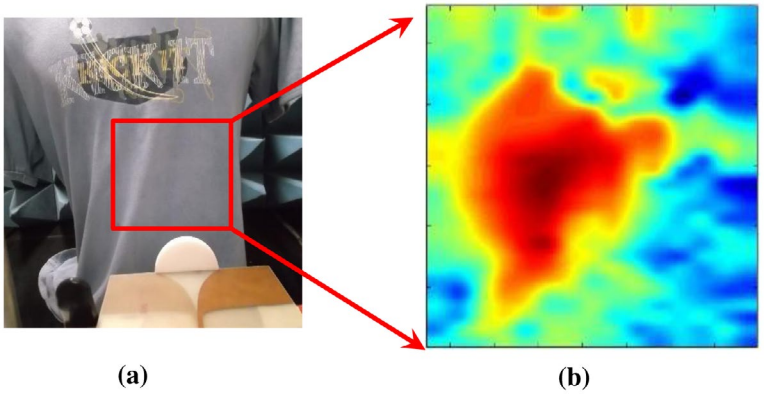

Figure 16. (a) Mannequin concealed with gun shaped metal object. (b) The corresponding reflectivity image obtained using the proposed technique.

band of operation. The concept of a hemisphere dielectric lens has been introduced, which is found to increase the overall directivity of the designed antenna. The designed antenna is superior in the terms of directivity, input reflection coefficient, the radiation pattern and the gain. Finally, the designed antenna along with the proposed time domain microwave imaging algorithms has been used to investigate various real-life contraband detection problems. The designed hemisphere-loaded Vivaldi antenna has shown potential for a number of microwave imaging applications because of its wide bandwidth and focusing capability.

Disclosure statement

No potential conflict of interest was reported by the authors.

Funding

Science and Engineering Research Board, Department of Science and Technology, India [grant number SB/S3/EECE/126/2013].

References

[1] Sheen DM, McMakin DL, Hall TE. Three-dimensional millimeter-wave imaging for concealed weapon detection. IEEE Trans. Microwave Theory Tech. 2001;49:1581–1592.

[2] Wong D, Carin L. Analysis and processing of ultra-wide-band SAR imagery for buried landmine detection. IEEE Trans. Antennas Propag. 1998;46:1747–1748.

[3] Yang Y, Fathy AE. See-through-wall imaging using ultra-wideband short-pulse radar system. In: IEEE International Symposium Antennas and Propagation Society; Jul 3–8; Washington, DC, USA; 2005.

[4] Akhtar MJ, Omar AS. A generalized technique for the reconstruction of permittivity profiles with a controllable resolution in an arbitrary coordinate system. IEEE Trans. Antennas Propag. 2005;53:294–304.

[5] Ahmed SS, Schiessl A, Gumbmann F, et al. Advanced microwave imaging. IEEE Microwave Mag. 2012;13:26–43.

[6] Gibson PJ. The Vivaldi Aereal. In: 9th European Microwave Conference; Sept 17–20; Brighton, UK; 1979.

[7] Huang W, Kishk AA. Compact dielectric resonator antenna for microwave breast cancer detection. IET Microwaves Antennas Propag. 2009;3:638–644.

[8] Yang Y, Wang Y, Fathy AE. Design of compact Vivaldi antenna arrays for UWB see through wall applications. Prog. Electromagnet. Res. 2008;82:401–418.

[9] Chiappe M, Gragnani GL. Vivaldi antennas for microwave imaging: theoretical analysis and design considerations. IEEE Trans. Instrum. Meas. 2006;55:1885–1891.

[10] Gazit E. Improved design of the Vivaldi antenna. IEE Proceedings H Microwaves, Antennas and Propagation. 1988;135:89–92.

[11] Akhtar MJ. Microwave imaging: reconstruction of permittivity profiles. Magdeburg: Vdm Verlag Dr. Mueller; 2008.

[12] Hood AZ, Karacolak T, Topsakal E. A small antipodal Vivaldi antenna for ultra-wideband applications. IEEE Antennas Wirel. Propag. Lett. 2008;7:656–660.

[13] Jian B, Shi S, Prather DW. Modified compact antipodal Vivaldi antenna for 4–50-GHz UWB application. IEEE Trans. Microwave Theory Tech. 2011;59:1051–1057.

[14] Zhou B, Cui T-J. Directivity enhancement to Vivaldi antennas using compactly anisotropic zero-index metamaterials. IEEE Antennas Wirel. Propag. Lett. 2011;10:326–329.

[15] Wang Y-W, Wang GM, Zong B-F. Directivity improvement of Vivaldi antenna using double-slot structure. IEEE Antennas Wirel. Propag. Lett. 2013;12:1380–1383.

[16] Abhijith, BN, Akhtar, MJ. Optimization of Vivaldi antenna for microwave imaging applications. In: IEEE Antennas and Propagation Society International Symposium; Jul 6–11; Memphis, Tennessee, USA; 2014.

[17] Akhter Z, Akhtar MJ. Time domain microwave technique for dielectric imaging of multi-layered media. J. Electromagn. Waves App. 2015;29:386–401.

[18] Caorsi S, Stasolla M. A layer stripping approach for EM reconstruction of stratified media. IEEE Trans. Geosci. Remote Sens. 2014;52:5855–5869.

[19] Ahmed SS, Schiessl A, Schmidt LP. A novel fully electronic active real-time imager based on a planar multistatic sparse array. IEEE Trans. Microwave Theory Tech. 2011;59:3567–3576.

[20] Akhter Z, Barman BK, Akhtar MJ. Two-dimensional microwave imaging scheme to detect concealed objects. In: IEEE MTT-S International Microwave and RF Conference; Dec 14–16; Delhi, India; 2013.

[21] Abubakar A, Berg PMVD, Semenov SY. Two- and three-dimensional algorithms for microwave imaging and inverse scattering. J. Electromagn. Waves App. 2003;17:209–231.

[22] Caorsi S, Donelli M, Lommi A, et al. Location and imaging of two-dimensional scatterers by using a particle swarm algorithm. J. Electromagn. Waves App. 2004;18:481–494.

[23] Akhter Z, Akhtar MJ, Microwave imaging of lossy dielectric stratified media using quasi-numerical optimization technique. In: IEEE Conference on Antenna Measurements & Applications (CAMA); Nov 16–19; Antibes; 2014.

[24] 2013a. MATLAB-matrix laboratory. Available from: http://in.mathworks.com/products/matlab/